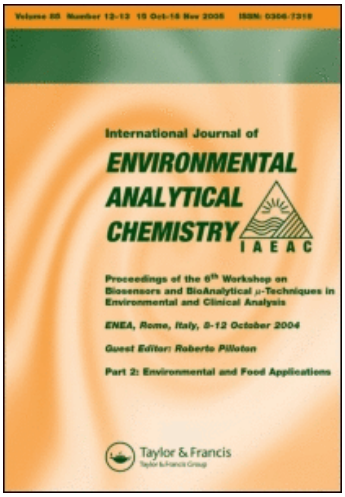

International Journal of Environmental Analytical Chemistry
Publication details, including instructions for authors and subscription information:
http://www.informaworld.com/smpp/title~content=t713640455

Light-induced transformations of fungicides on titanium dioxide: pathways and by-products evaluation using the LC-MS technique

Paola Calza[a]; Claudio Medana[a]; Claudio Baiocchi[a]; Ezio Pelizzetti[a]
[a] Dipartimento di Chimica Analitica, Università di Torino, 10125 Torino, Italy

To cite this Article Calza, Paola , Medana, Claudio , Baiocchi, Claudio and Pelizzetti, Ezio(2006) 'Light-induced transformations of fungicides on titanium dioxide: pathways and by-products evaluation using the LC-MS technique', International Journal of Environmental Analytical Chemistry, 86: 3, 265 — 275
To link to this Article: DOI: 10.1080/03067310500247959
URL: http://dx.doi.org/10.1080/03067310500247959

Intern. J. Environ. Anal. Chem.
Vol. 86, Nos. 3–4, 15 March–10 April 2006, 265–275

Taylor & Francis
Taylor & Francis Group

Light-induced transformations of fungicides on titanium dioxide: pathways and by-products evaluation using the LC-MS technique

PAOLA CALZA*, CLAUDIO MEDANA, CLAUDIO BAIOCCHI and EZIO PELIZZETTI

Dipartimento di Chimica Analitica, Università di Torino, via P. Giuria 5, 10125 Torino, Italy

(*Received 27 September 2004; in final form 6 May 2005*)

Azoxystrobin, carbendazim, and mepanipyrim, widely used heterocyclic fungicides, have been photocatalytically degraded in aqueous solution on TiO_2. Several concomitant pathways occur, concerning reductive and/or oxidative attacks, thus leading to numerous intermediates, identified and characterized through an MS^n spectra analysis. Multiple stage mass spectrometry of redox degradation compounds was simpler than that of parent fungicides, whose strong structures sometimes caused deactivated fragmentation pathways. Noteworthy were the different fragmentation ways that enabled hydroxylation positions to be located. Azoxystrobin is easily degraded and, within a few hours of irradiation, complete mineralization is achieved. For mepanipyrim and carbendazim, instead of an initial marked degradation, a lack in both carbon and nitrogen mineralization is observed. This is linked to the formation in both cases of guanidine, the only species persistently observed in the investigated time and still containing bound nitrogen.

Keywords: Fungicides; Azoxystrobin; Carbendazim; Titanium dioxide; Photocatalysis; HPLC/MS

1. Introduction

The persistence of pesticides in products destined for human consumption is of great concern, in particular because of their potential carcinogenic character. It is also of interest to identify the transformation products formed through their degradation and to evaluate their stability and toxicity, as well as to detect them with residues of the primary compound [1, 2].

*Corresponding author. Fax: +39-116707615. Email: paola.calza@unito.it

International Journal of Environmental Analytical Chemistry
ISSN 0306-7319 print: ISSN 1029-0397 online © 2006 Taylor & Francis
DOI: 10.1080/03067310500247959

For this purpose, in the present article we will examine the transformation pathways of several molecules belonging to different classes of pesticides. Some information about their transformations may be obtained, adopting a photocatalytic process. Photocatalytic degradation with irradiated semiconductors has been found to be effective for degradation and final mineralization of several organic compounds and in gaining information on naturally occurring transformations. This laboratory simulation has been successfully applied in previous studies [3, 4] and could be similarly utilized in the conditions used in the present study such as enlighting the photo-induced mechanism involving pesticide degradation.

In a previous study [5], it was found that the presence of a substructure –N–$C(NH_2)$=N– in the molecule leads to a negligible conversion of the organic nitrogen into inorganic ions in the period of investigation. In an attempt to clarify the possible transformation pathways followed by these species, we have examined and compared pesticides holding different substituents on this moiety: a phenyl group (mepanipyrim), methoxy carbonyl (carbendazim), or absence of the amino group (azoxystrobin). Azoxystrobin, (methyl-2-{2-[6-(2-cyanophenoxy) pyrimidin-4-yloxy] phenyl}-3-methoxyacrylate) is the more suitable pesticide among the strobilurins, a new class of fungicides active against a broad spectrum of fungi. Mepanipyrim (*N*-(4-methyl-6-prop-1-ynilpyrimidin-2-yl)aniline) belongs to the pyrimidinic class, while carbendazim (methyl benzimidazol-2-yl carbamate) is the most widely used active ingredient in the benzimidazole carbamate class of fungicides; it is very persistent in water, wastewater, soil, and food. Carbendazim is not only an extensively used fungicide but also the major metabolic product of other benzimidazole fungicides such as benomyl and thiophanate-methyl [6–8]. All these fungicides are active against a broad spectrum of fungi and are commonly adopted in agriculture, above all in wheat, grapes, fruit, and vegetable treatments [9–14]. The environmental persistence of fungicides has been reported in the literature [15].

The more suitable techniques for detection of the initial pesticides and their transformation products are the hyphenated techniques [16, 17], so our experiments were performed using an HPLC/MS^n instrument.

2. Experimental

Mepanipyrim, carbendazim, azoxystrobin (Dr. Ehrenstorfer), and guanidine (Aldrich) were used as received. Sodium sulphate (Aldrich), ammonium chloride (Carlo Erba), potassium nitrate (Merck), and sodium nitrite (Carlo Erba) were used after drying. HPLC-grade water was obtained from MilliQ System Academic (Waters, Millipore). Methanol HPLC grade (BDH) was filtered through a 0.45 μm filter before use. Ammonium acetate reagent grade was purchased from Fluka.

All experiments were carried out using TiO_2 Degussa P25 as the photocatalyst. The irradiations were performed using a 1500 W xenon lamp (Solarbox, CO.FO.MEGRA, Milan), simulating AM1 solar light, and equipped with a 340 nm cutoff filter. The irradiation was carried out on 5 mL of suspension containing 15 mg L^{-1} of pesticide and 200 mg L^{-1} of TiO_2. The pesticide concentration was chosen as a trade-off between solubility and sensitivity, while an excess of catalyst was used. The entire content of the cell was filtered through a 0.45 μm filter and then analysed by the appropriate analytical technique.

2.1 *Analytical procedures*

2.1.1. HPLC-MS. The chromatographic separations were run on a C18 column Phenomenex Luna, 150×2.0 mm (Chrompack, The Netherlands). The injection volume was 10 μL, and the flow rate was 200 μL min^{-1}. Gradient mobile phase composition was adopted: 0/100 to 30/70 in 25 min for methanol/aqueous ammonium acetate 15 mM pH 6.8. An LCQ DECA XP Plus ion trap mass spectrometer (ThermoFinnigan) equipped with an atmospheric pressure interface and an ESI ion source was used. The LC column effluent was delivered into the ion source using nitrogen as a sheath and auxiliary gas (Claind Nitrogen Generator apparatus). The source voltage was set at 4.5 kV. The heated capillary value was maintained at 300°C. The acquisition method used was previously optimized in the tuning sections for the parent compound (capillary, magnetic lenses, and collimating octapole voltages) in order to achieve maximum sensitivity. The tuning parameters adopted for ESI source were as follows: source current 5.00 μA, capillary voltage 11.00 V, capillary temperature 300°C, tube lens −20 V; for ion optics, multipole 1 offset −6.75 V, inter-multipole lens voltage −16.00 V, multipole 2 offset −10.50 V.

2.1.2. Ion chromatography. A Dionex instrument was employed, equipped with a conductimeter detector. The determination of ammonium ions was performed by adopting a column CS12A and 25 mM metansulphonic acid as eluant and a flow rate of 1 mL min^{-1}. Under such conditions, the retention time is 4.7 min. The anions were analysed using an AS9HC anionic column and a mixture of 12 mM $NaHCO_3$ and 5 mM K_2CO_3 at a flow rate of 1 mL min^{-1}. Under such experimental conditions, the retention times were 4.3, 6.63, and 9.58 min for acetic acid, nitrite, and nitrate, respectively.

2.1.3. Total carbon analyser. Total organic carbon (TOC) was measured on filtered suspensions using a Shimadzu TOC-5000 analyser (catalytic oxidation on Pt at 680°C). Calibration was achieved by injecting standards of potassium phthalate.

3. Results and discussion

In the present study, the investigated fungicides were irradiated using titanium dioxide as a photocatalyst. The principles of heterogeneous photocatalytic processes have been widely described in the literature [18–20]. Light excitation promotes the formation of electron–hole couples, which can recombine with heat dissipation. Dissipation is prevented by migration of both active species toward the semiconductor surface, where electrons can be trapped by surficial Ti^{IV} ions to give Ti^{III}, while holes can be trapped by –OH surface groups (as adsorbed $^{\bullet}OH$) and by sub-superficial O_2^- (as $^{\bullet}O^-$). The photodecomposition of the pesticides could thus be carried out by oxidative or reductive species.

Both the disappearance of the initial compound and the evolution of intermediates have been monitored by HPLC-MS^n analysis of solutions after various irradiation times. In the following, the different pesticides are presented separately by paying attention to the MS analysis of the initial molecules, very useful in confirming

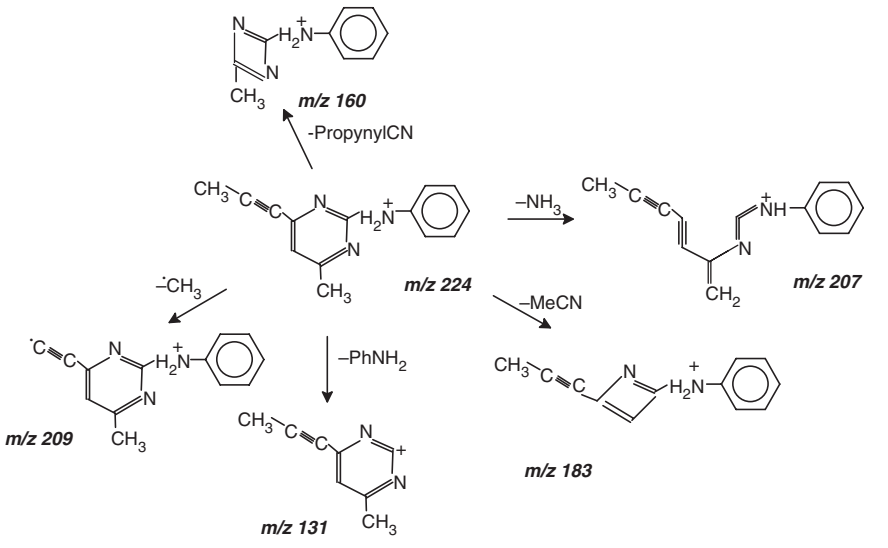

Scheme 1. Fragmentation pathway followed by mepanipyrim.

their presence in the environment and in attributing a structure to unknown compounds formed during pesticide degradation, and to the formation of intermediates.

3.1 *Mepanipyrim*

3.1.1. MS study. From an examination of the mepanipyrim fragmentations shown in scheme 1 allows, we can pick out many substituent differences existing in redox derivatives, and these have been carefully considered in identifying the unknown intermediates. This molecule requires a high collision energy for fragmentation, probably because of the extended conjugation near this structure. In the absence of common neutral elimination from MH^+, usually deactivated fragmentation pathways as radical losses (MH^+–$CH_3^{\bullet}$, m/z 209, base peak) or extended rearrangement (MH^+–NH_3, m/z 207) take place. In addition, the cleavage of C–N and C–C bonds, together with ring contraction, occurs with the release of a MeCN or a PrCN molecule (fragments m/z 183 and 160).

The common aniline elimination, typical of many pesticide compounds, generates a minor but significant product ion (m/z 131).

3.1.2. Photo-induced degradation. Various species have been recognized, characterized by different m/z ratios along with several peaks corresponding to an equal m/z value and have been characterized through a deep MS spectra analysis, as described elsewhere [21].

The early steps proceed through an oxidative process, with the formation of the hydroxylated (MW 239) and bihydroxylated (MW 255) intermediates (see pathway 1 in scheme 2), or alternative pathways, arising from the concerted oxidative and reductive attacks on the triple bond and leading to the formation of the species holding MW 243 (pathway 2) and 241 (pathway 3).

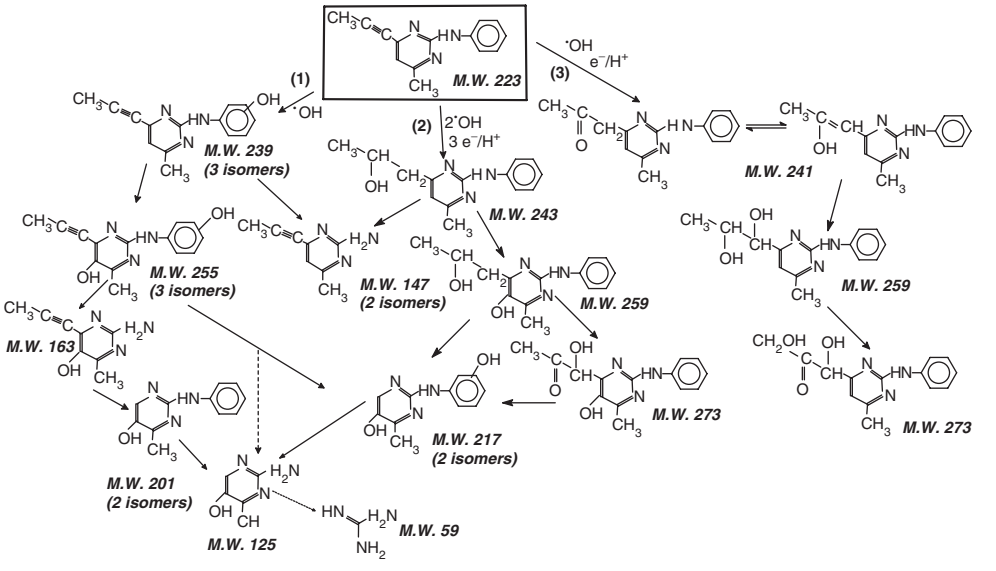

Scheme 2. Main transformation pathways involved in the mepanipyrim photo-induced transformation.

Afterwards, various competitive pathways can occur, thus leading to a wide range of intermediates, as shown in scheme 2. With the reductive steps being confined to the propynylic chain, the further transformation pathways of all early species formed from both oxidative and oxido/reductive steps follow the same reaction steps. These involve: (1) the cleavage of the C–C bond with the release of the propynylic chain (with the formation of the structures at MW 217 and 201) and/or (2) cleavage of the C–N bond with the detachment of benzenic moiety as phenol, hydroquinone, or cathecol on one side and the formation of a structure at MW 147 and 163 on the other side.

All identified aromatic structures are completely degraded up to 30 min of irradiation [21]. As far as their degradation is concerned, the TOC profile shows a remarkable decrease up to 30 min (figure 1), while a small yield of organic carbon is also observed after 120 min of irradiation; this is predominantly attributed to guanidine formation. Kinetically, it is the last species formed, and it is persistently observed in the considered time, in agreement with the high photocatalytic stability found in previous studies [5].

In the experiment, the organic carbon was mostly transformed into CO_2, and a large amount of the organic nitrogen was still bound. Only a small yield was released, mainly as ammonium ions, through a mechanism well documented in literature [22–24].

3.2 *Carbendazim*

3.2.1. MS study. The main fragmentation pathways elaborated on the basis of MS^n spectra analysis are depicted in scheme 3. From MS^2 fragmentation, the daughter ion at m/z 160 is formed through the loss of a methanol molecule, followed by the formation of the ion at m/z 132, through the loss of a CO molecule. Through a ring-contraction rearrangement, the ion at m/z 105 is formed though the loss of 27 amu (HCN).

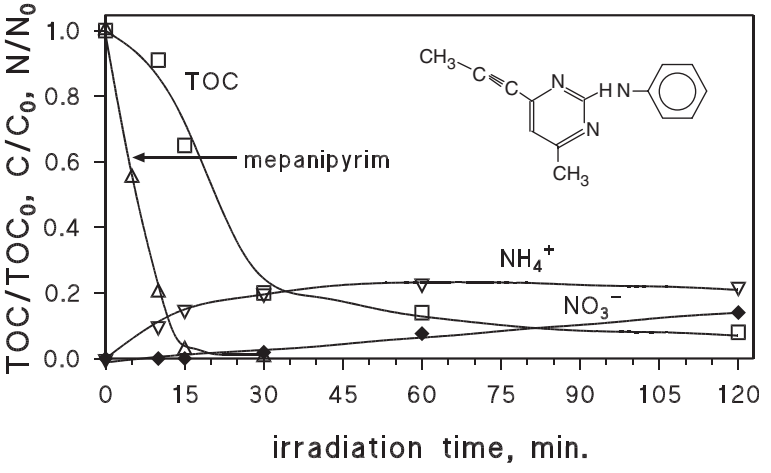

Figure 1. Degradation of mepanipyrim on 200 mg L^{-1} of TiO_2; disappearance of initial compound, TOC profile, and evolution of ammonium and nitrate ions.

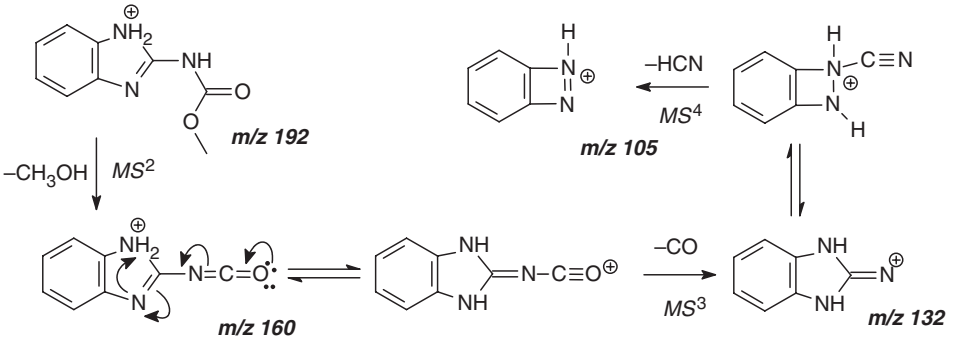

Scheme 3. Fragmentation pathway followed by carbendazim.

3.2.2. Photo-induced degradation. Carbendazim is easily degraded ($t_{1/2}$ 4 min, see figure 2), and the transformation products summarized in figure 3 are formed (see scheme 4 also). Analogous to what was observed under homogeneous photolysis [25], in the presence of TiO_2, breakage of the hetero-ring occurs with the concomitant formation of methoxycarbo-guanidine and dihydroxybenzene. Even if carbomethoxy-guanidine is very stable to homogeneous photolysis [25], it is rapidly degraded (see figure 3) and transformed into guanidine on one side, and acetic acid on the other side.

Further transformation of these intermediates occurs with very different rates. Acetic acid is completely mineralized up to 2 h of irradiation, while a different fate applies for guanidine, the same final degradation product observed from mepanipyrim degradation. The analogy between these two structures lies in the N–C(NHR)=N moiety, whose detachment leads to the formation of guanidine. As can be deduced from figure 2, a TOC residual remains (~10%), and a lack in the stoichiometric release of organic nitrogen is observed. It will be mineralized only after a long irradiation time (70 h), mainly as nitrate ions [5].

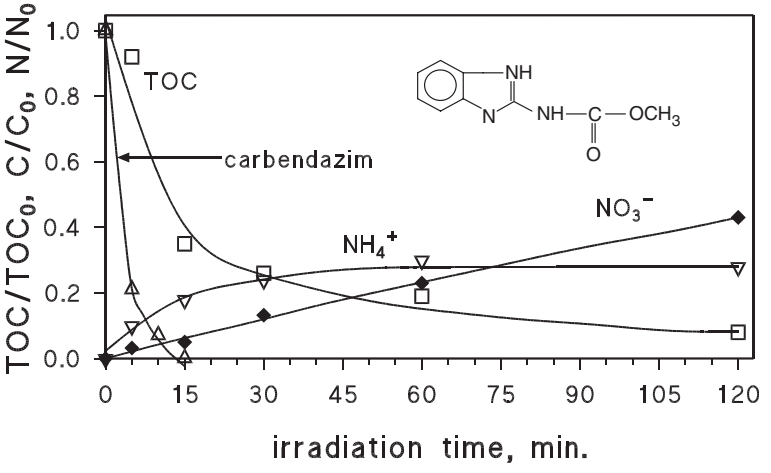

Figure 2. Degradation of carbendazim on 200 mg L^{-1} of TiO_2; disappearance of initial compound, TOC profile, and evolution of ammonium and nitrate ions.

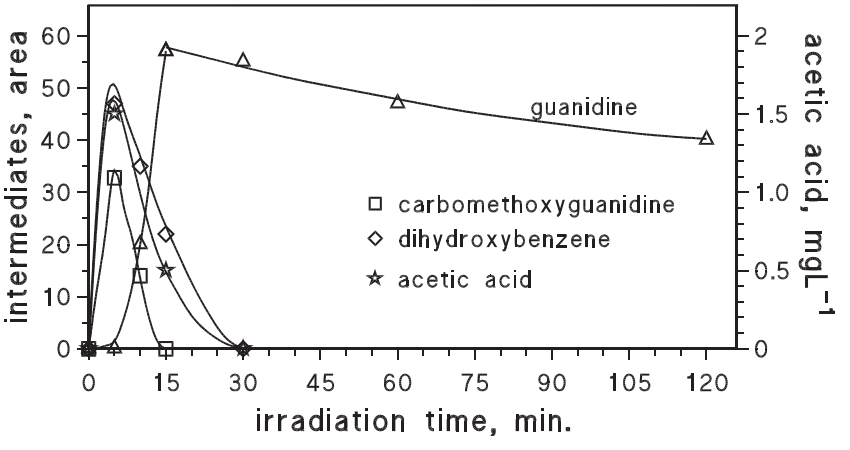

Figure 3. Evolution of intermediates formed during carbendazim transformations as a function of irradiation time. Carbomethoxy-guanidine, guanidine, and dihydroxybenzene are expressed as peak area ($\times 10^{-6}$), while acetic acid is expressed as concentration.

3.3 *Azoxystrobin*

3.3.1. MS study. Azoxystrobin multiple-stage fragmentations are shown in scheme 5. The presence of two methoxy groups allows different methanol losses to take place. One of the isomeric ions with *m*/*z* 372 could be described with a structure which easily loses methoxyacetylene or carbon dioxide. From the latter structure, a methoxy radical leaves the ion generating the species with *m*/*z* 329.

3.3.2. Photo-induced transformation. Azoxystrobin photocatalytic degradation is shown in figure 4. Numerous intermediates have been identified. The initial degradation intermediates are essentially oxidation products, as shown in scheme 6. Two

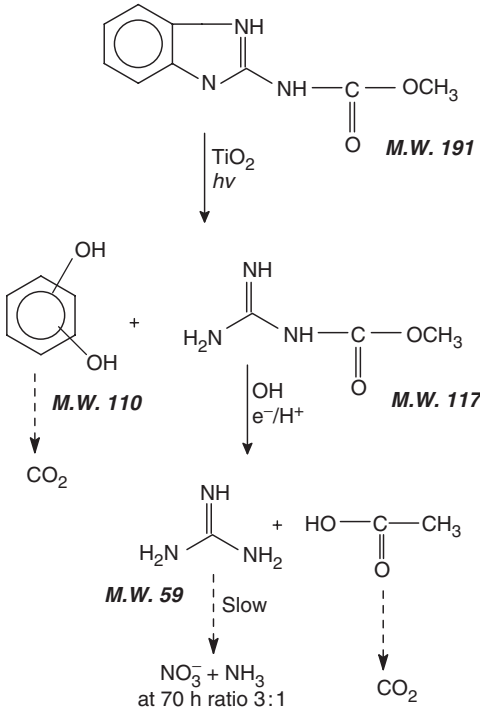

Scheme 4. Main transformation pathways involved in the carbendazim photo-induced degradation.

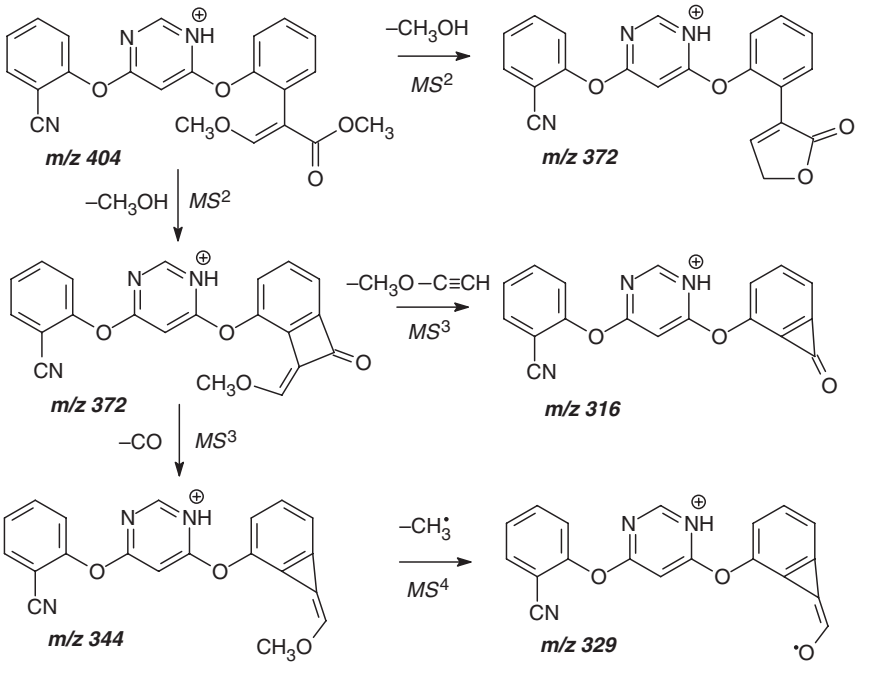

Scheme 5. Fragmentation pathways followed by azoxystrobin.

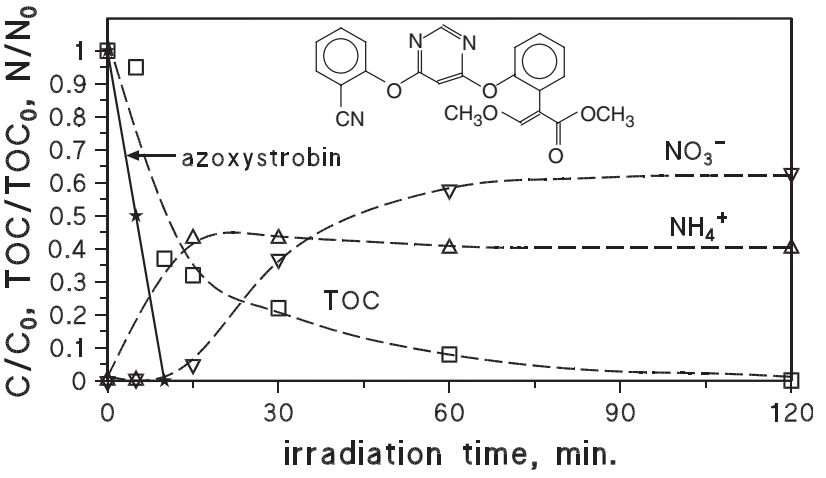

Figure 4. Degradation of azoxystrobin 15 mg L^{-1} on 200 mg L^{-1} of TiO_2; disappearance of initial compound, TOC profile, and evolution of ammonium and nitrate ions.

hydroxylated derivates are formed, with *m*/*z* 220, and attributed to the structures I and II, via hydroxylation of the cyanophenyl ring at the 8- and 10-position, in agreement with the hydroxy derivatives found in metabolic studies on rats [26]. A second parallel pathway occurs, leading to the oxidation of the methylic groups into an aldehydic group and attributed to the structures indicated in scheme 6 (structure III). Another transformation pathway involves the acrylate moiety, resulting in the formation of the des-methoxy-methenyl-azoxystrobin (see structure IV) and its hydroxylated derivative (structure V).

A further transformation arises from the cleavage of the ether linkage between the cyanophenyl and pyrimidinyl rings, giving structure VI. All these intermediates are easily degraded themselves, as shown in figure 5. Differently to the other two pesticides through the ring-opening with the formation of aliphatic compounds, complete mineralization is achieved within two hours of irradiation.

Organic nitrogen is also easily released and, after 2 h of irradiation, nitrate and ammonium ions are formed in stoichiometric amount (see figure 4). The different fate followed by azoxystrobin is linked to the substitution of the NHR group in the N–C(NHR)=N moiety with a CH_2 group. This high stability observed above is then lost, so that the complete abatement is achieved. The CN group is mainly transformed into nitrate ions [27], while both nitrate and ammonium ions are formed from the N–CH=N moiety.

4. Conclusions

The pesticides investigated here have been shown to be easily reduced by a photocatalytic process, and through a reductive and/or oxidative attack sequence, several intermediates have been formed. These transformation products are themselves degraded, so in the case of azoxystrobin, complete mineralization is achieved. In contrast, carbendazim and mepanipyrim show a lack of mineralization, due to the

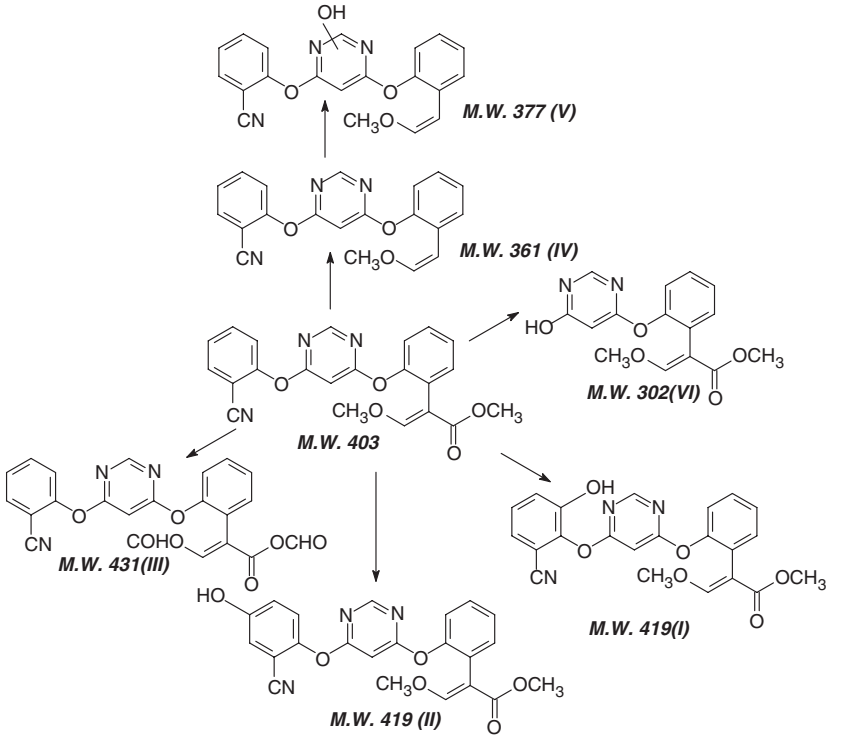

Scheme 6. Main transformation pathways involved in the azoxystrobin photo-induced degradations.

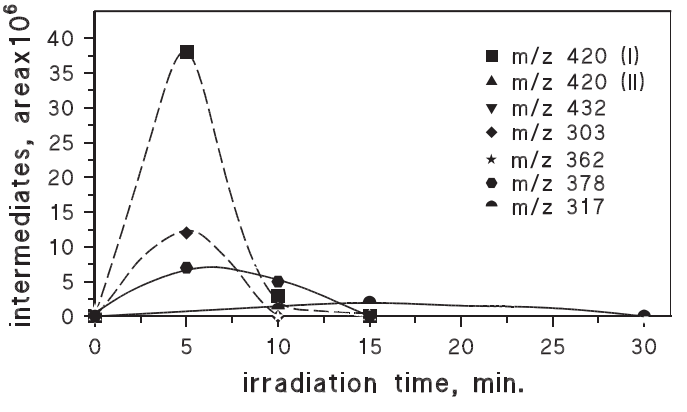

Figure 5. Evolution of intermediates formed from azoxystrobin transformation as a function of irradiation time.

formation of guanidine as a final intermediate, a very stable compound that does not permit in the investigated time the release of nitrogen as inorganic ions and complete mineralization.

The intermediates identified match those found in the metabolic study, when available, and several new species have been found in this laboratory simulation, that could be formed in treated vegetables.

References

[1] V.L. Garau, A. Angioni, A.A. Del Real, M. Russo, P. Cabras. *J. Agric. Food Chem.*, **50**, 1929 (2002).
[2] P. Cabras, A. Angioni, V.L. Garau, F.M. Pirisi, J. Espinosa, A. Mendoza, F. Cabitza, M. Pala, V. Brandolini. *J. Agric. Food Chem.*, **46**, 3249 (1998).
[3] S.Y. Panshin, D.S. Carter, E.R. Bayless. *Environ. Sci. Technol.*, **34**, 2131 (2000).
[4] P. Calza, C. Medana, M. Pazzi, C. Baiocchi, E. Pelizzetti. *J. Pharm. Biomed. Anal.*, **35**, 9 (2004).
[5] P. Calza, C. Medana, C. Baiocchi, E. Pelizzetti. *Appl. Catal. B: Environ.*, **52**, 267 (2004).
[6] S.A. Sassman, L.S. Lee, M. Bischoff, R.F. Turco. *J. Agric. Food Chem.*, **52**, 747 (2004).
[7] A. Veneziano, G. Vacca, S. Arana, F. De Simone, L. Rastrelli. *Food Chem.*, **87**, 383 (2004).
[8] S. Radice, L. Marabini, M. Gervasoni, M. Ferraris, E. Chiesara. *Toxicology*, **123**, 135 (1997).
[9] M. Ikeda, Y. Asano, Y. Maeda, Y. Yusa. *J. Pestic. Sci.*, **23**, 1 (1998).
[10] Y. Nagai, K. Shimba, Y. Yaga, A. Yagi. *J. Pestic. Sci.*, **24**, 280 (1999).
[11] D.H. Huston, T.R. Roberts, P.J. Jewess. In *Metabolic Pathways of Agrochemicals Part 2. Insecticides and Fungicides*, D.H. Huston, T.R. Roberts (Eds), pp. 1120–1132, Royal Society of Chemistry, Cambridge, UK (1999).
[12] D.W. Bartlett, J.M. Clough, J.R. Godwin, A.A. Hall, M. Hamer, B. Parr-Dobrzanski. *Pestic. Manag. Sci.*, **58**, 647 (2002).
[13] S. Hayashi, S. Maeno, T. Kimoto, T. Nagata. *J. Pestic. Sci.*, **22**, 165 (1997).
[14] T. Anesiadis, G.S. Karaoglanidis, K. Tzavella-Klonari. *J. Phytopathol.*, **151**, 647 (2003).
[15] A.G. Hornsby, T.M Buttler, R.B. Brown. *Agric. Ecosyst. Environ.*, **46**, 187 (1993).
[16] H.B. Christensen, K. Granby. *Food Addit. Contam.*, **18**, 866 (2001).
[17] A. Sannino, L. Bolzoni, M. Bandini. *J. Chromatogr. A*, **1036**, 161 (2004).
[18] D.W. Bahnemann, J. Fox, E. Pelizzetti, P. Pichat, N. Serpone. In *Aquatic and Surface Photochemistry*, G.R. Helz, R.G. Zepp, D.G. Crosby (Eds), pp. 261–316, Lewis, Boca Raton, FL (1994).
[19] C. Minero, G. Mariella, V. Maurino, E. Pelizzetti. *Langmuir*, **16**, 2632 (2000).
[20] M.A. Fox, M.T. Dulay. *Chem. Rev.*, **93**, 341 (1993).
[21] P. Calza, C. Medana, C. Baiocchi, P. Branca, E. Pelizzetti. *J. Chromatogr. A*, **1049**, 115 (2004).
[22] R. Terzian, N. Serpone, C. Minero, E. Pelizzetti. *J. Catal.*, **128**, 352 (1991).
[23] V. Maurino, C. Minero, E. Pelizzetti, P. Piccinini, N. Serpone, H. Hidaka. *J. Photochem. Photobiol. A: Chem.*, **109**, 171 (1997).
[24] S. Horikoshi, N. Watanabe, M. Mukae, H. Hidaka, N. Serpone. *New J. Chem.*, **25**, 999 (2001).
[25] A. Boudina, C. Emmelin, A. Baaliouamer, M.F. Grenier-Loustalot, J.M. Chovelon. *Chemosphere*, **50**, 649 (2003).
[26] W.J.D. Laird, A.J. Gledhill, G.J. Lappin. *Xenobiotica*, **33**, 677 (2003).
[27] P. Calza, E. Pelizzetti, C. Minero. *J. Appl. Electrochem.*, **35**, 665 (2005).